

Supporting Information

Polydopamine-modulated covalent organic framework membranes for molecular separations

Jianliang Shen,^{ab} Runnan Zhang,^{*ab} Yanlei Su^{ab}, Benbing Shi,^{ab} Xinda You,^{ab} Weixiong Guo,^{ab} Yu Ma,^{ab}
Jinxiu Yuan,^{ab} Fei Wang^{ab} and Zhongyi Jiang^{*ab}

^a Key Laboratory for Green Chemical Technology, School of Chemical Engineering and Technology, Tianjin University, Tianjin 300072, China

^b Collaborative Innovation Center of Chemical Science and Engineering (Tianjin), Tianjin, 300072, China

* E-mail: runnan.zhang@tju.edu.cn Tel: 86-22-23500086, Fax: 86-22-23500086

* E-mail: zhyjiang@tju.edu.cn Tel: 86-22-23500086, Fax: 86-22-23500086

2. Experimental section

2.1 Preparation of SCOF/PDA/PAN membranes

The preparation procedure of PDA/PAN supports was described in detail in our manuscript. The resultant PDA(1)/PAN supports were immersed into COF building monomer solution containing different concentrations of DABA and TFP monomers, and the reaction was conducted for 72 h at room temperature (25 °C). The resultant membranes, designated as SCOF/PDA(1)/PAN membranes, were washed with 1,4-dioxane, ethanol and DI water several times and were used for further characterization.

2.2 Preparation of modified PDA/PAN supports

DABA (9 mmol/L) and TFP (6 mmol/L) were dissolved in 12.5 mL DI water and 1,4-dioxane, respectively. Then PDA(1)/PAN support was immersed into DABA solution followed by adding 12.5 mL 1,4-dioxane. Likewise, another PDA(1)/PAN support was immersed into TFP solution followed by adding 12.5 mL DI water. The PDA(1)/PAN supports were left in the mixture at room temperature. After 72 h, the PDA(1)/PAN supports were taken out and air-dried for further characterization.

Table S1 SCOF/PDA(1)/PAN membranes prepared with different COF monomer concentrations.

Membrane	PDA deposition time (h)	COF building monomers	
		DABA concentration (mmol/L)	TFP concentration (mmol/L)
1#	1.0	2.4	1.6
2#	1.0	6.0	4.0
3#	1.0	9.0	6.0
4#	1.0	12.0	8.0
5#	1.0	24.0	16.0

2.3 Membrane characterization

ATR-FTIR analysis. Attenuated total reflectance Fourier transform infrared spectroscopy spectrophotometer (ATR-FTIR, Nicolet 560, USA) was utilized to analyze the chemical structure of the monomer modified PAN(1)/PAN supports with a scanning wavelength in the range of 4000-400 cm^{-1} .

Element distribution measurement. Energy-dispersive X-ray spectroscopy (EDX, Genesis XM2 APEX 60SEM, USA) was employed to measure the element distribution of PDA/PAN supports and SCOF/PDA/PAN membranes.

Pore size distribution measurement. The pore size distribution of SCOF/PDA/PAN membrane was calculated from N_2 sorption isotherms at 77 K using gas adsorption analyzer (Quantachrome Autosorb-IQ, America).

Compacting-resistant test. In order to measure the compacting-resistant of the SCOF/PDA/PAN membranes, the pure water flux ($\text{L m}^{-2} \text{h}^{-1}$) of membranes under different operating pressure (0.05-0.35 MPa) was tested.

XRD analysis. The X-ray diffractometer (XRD) pattern of SCOF/PAN membrane was recorded on a D/MAX-2500 X-ray diffractometer (Cu $\text{K}\alpha$) at room temperature, and every XRD pattern was conducted at 2θ angles range from 3° - 35° with a rate of $1^\circ/\text{min}$.

SEM analysis. Cross-sectional morphologies of the PAN and PDA/PAN support were conducted on a scanning electron microscopy (SEM, Nanosem 430, Japan).

Dye adsorption measurement. The adsorption test of Eriochrome black T by SCOF/PDA(1)/PAN membrane was studied as well. SCOF/PDA(1)/PAN membrane was immersed in the filtration device (Amicon 8050, Millipore, USA) filled with 30 mL Eriochrome black T solution (100 ppm). After 120-h static adsorption at room temperature (25 °C), the concentration before and after adsorption were measured with UV-vis spectrophotometer (Hitach UV-2800, Hitach Co., Japan).

Chemical stability measurement. In order to assess the chemical stability of the SCOF/PDA/PAN membrane in acidic/alkaline environment, membrane samples were immersed in HCl (pH=1) and NaOH (pH=11) aqueous solution for 168 h, respectively. Then the performance of the treated membranes were measured and compared with those of the pristine ones after DI water rinsing. (Testing condition: 100 ppm dye solutions at 0.1 MPa; 13.4 cm^2 effective membrane area; 25 °C; each above value was based on the average of at least three independent samples)

3. Results and discussion section

3.1 Formation mechanism of PDA/PAN support

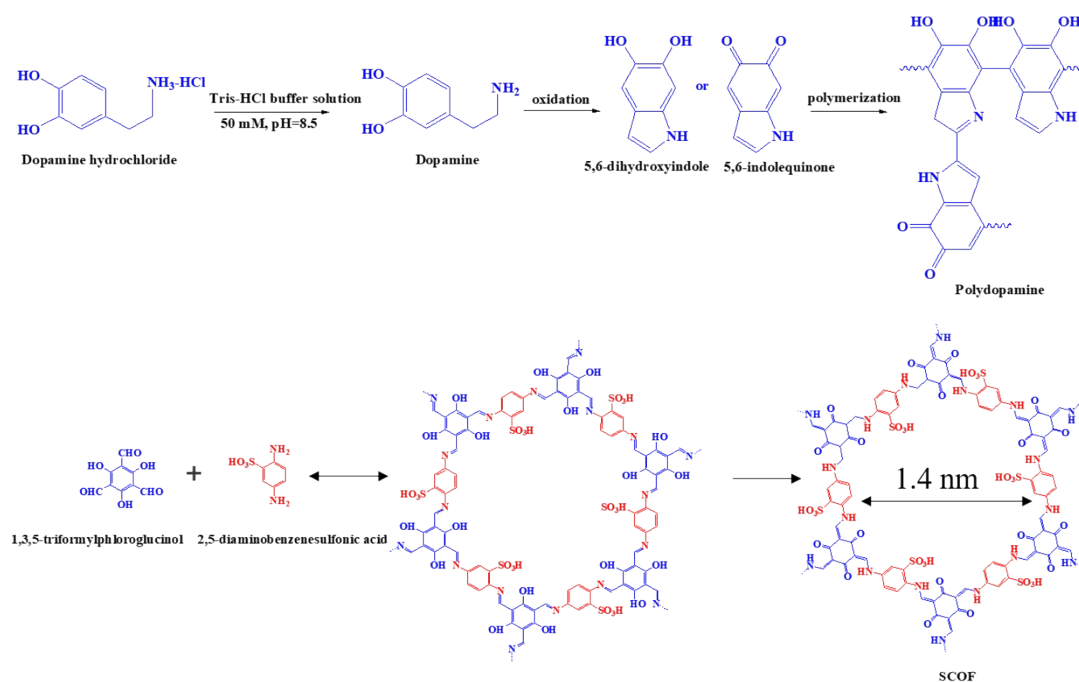


Fig. S1. The probable reaction routes in this work.

New peaks shown between 3300 cm^{-1} and 3500 cm^{-1} corresponded to amino groups. The peaks shown at 1026 cm^{-1} corresponded to O=S=O stretching band. The results indicated the DABA monomer was adsorbed to the surface of PDA/PAN support. The peak at 1643 cm^{-1} corresponding to C=O stretching band implying the TFP monomer was attracted to the support.

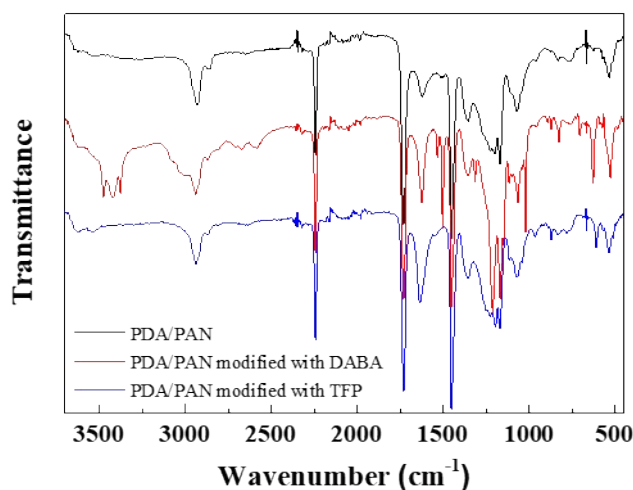


Fig. S2. ATR-FTIR spectrum of PDA(1)/PAN support, PDA(1)/PAN support modified with DABA and PDA(1)/PAN support modified with TFP.

As shown in Fig. S3, the color of the SCOF/PAN membrane was lighter than that of SCOF/PDA(1)/PAN membrane, indicating few SCOF crystallites formation on unmodified PAN surface. It was reported that the XRD peaks of the COF layer could be obviously observed only when the thickness of the layer was thick enough ($\sim 100\text{ }\mu\text{m}$)^[S1-S3]. Thus, the crystallinity of SCOF/PAN membrane was lower than that of SCOF/PDA(1)/PAN membrane.

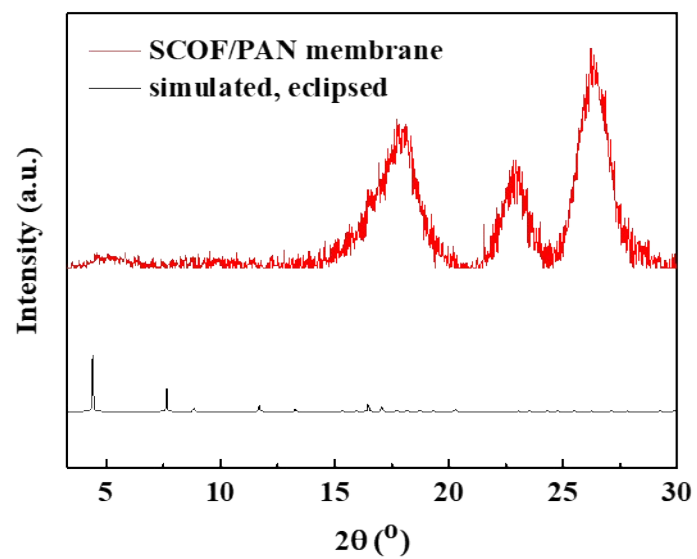


Fig. S3 XRD pattern of simulated SCO and as-synthesized SCO/PAN membrane.

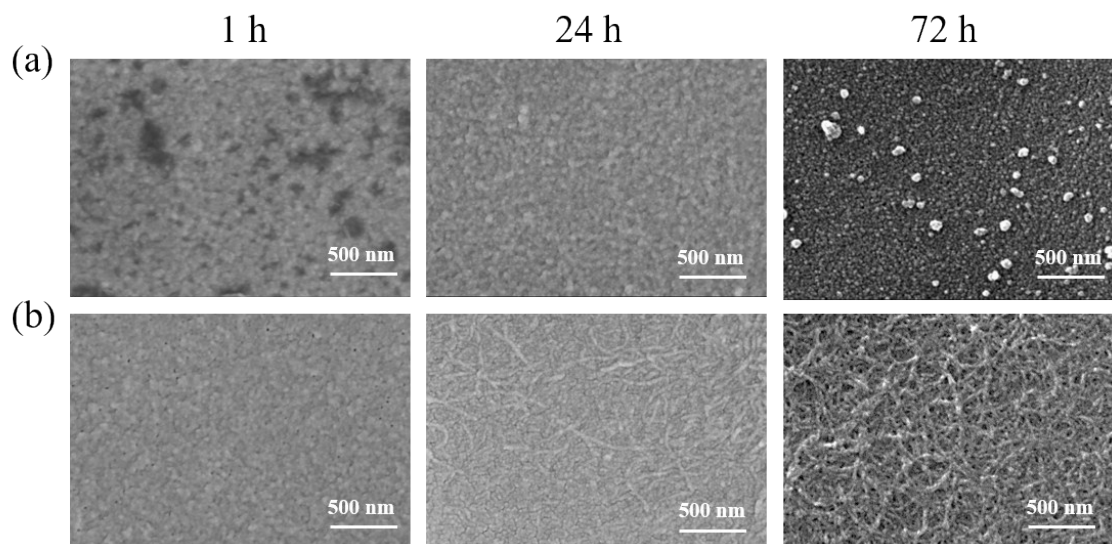


Fig. S4 Surface SEM images of the (a) SCO/PDA(1)/PAN membranes and (b) SCO/PAN membranes with different reaction time.

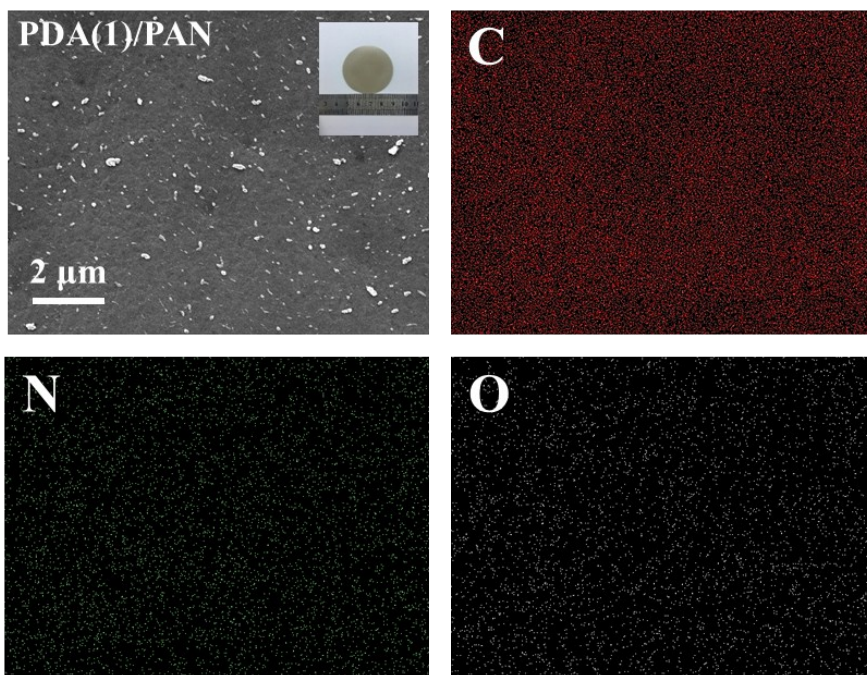


Fig. S5 The SEM image of PDA(1)/PAN support and EDX C, N, O element mapping (Inset: the photographs of PDA(1)/PAN support).

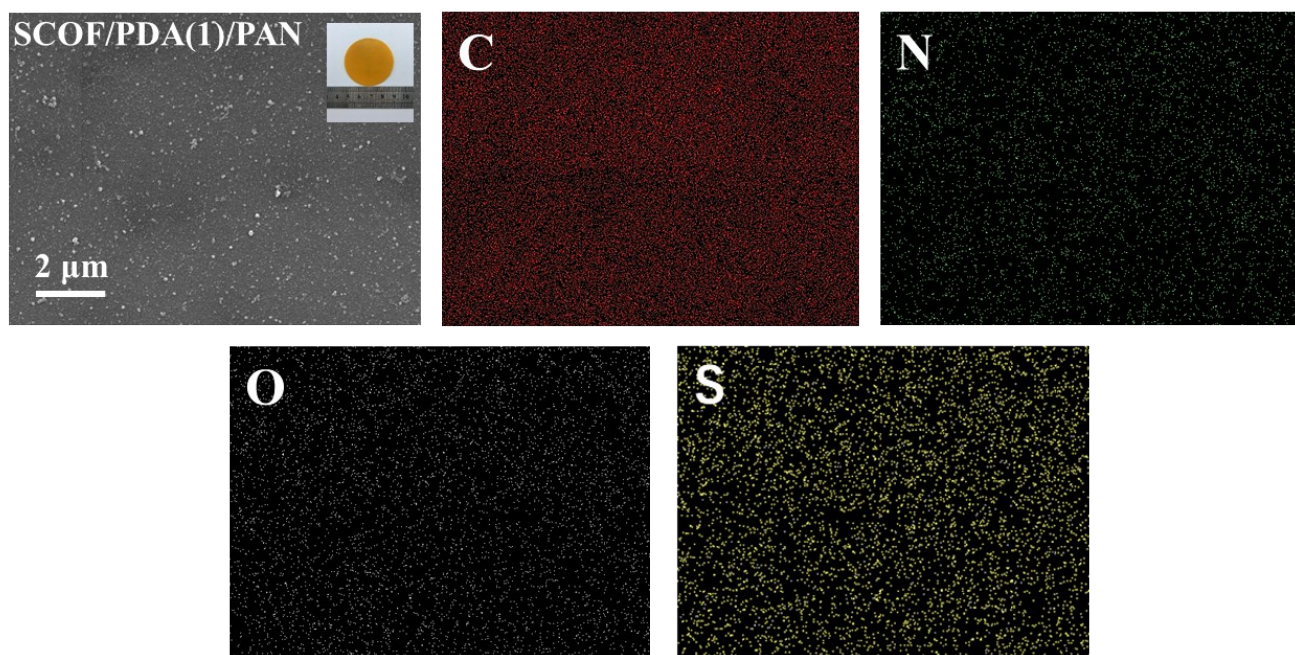


Fig. S6 The SEM image of SCOF/PDA(1)/PAN membrane (3#) and EDX C, N, O, S element mapping (Inset: the photographs of membrane 3#).

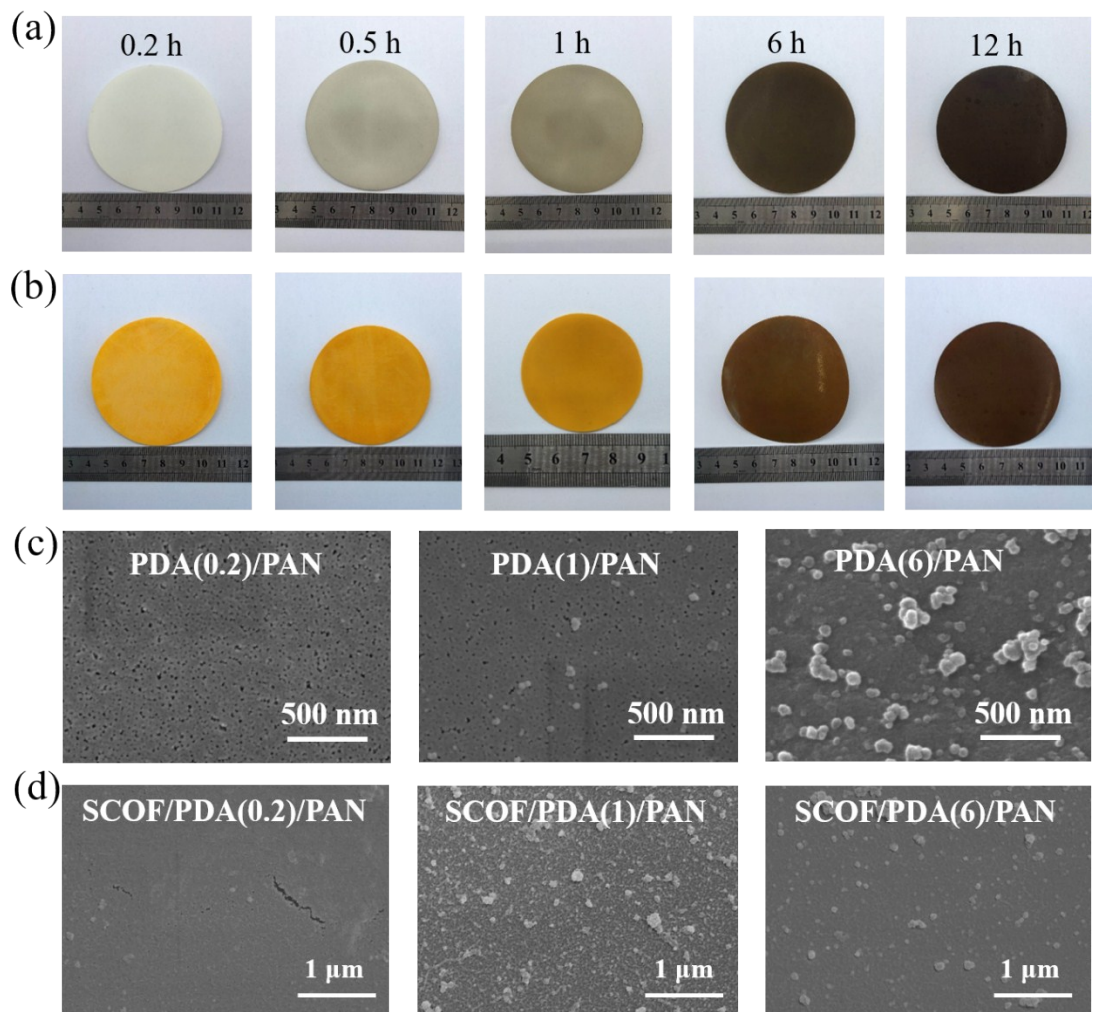


Fig. S7 Digital photographs of (a) PDA/PAN supports; (b) SCOF/PDA/PAN membranes with different PDA deposition time. PDA deposition time from left to right: 0.2 h, 1 h, 6 h; (c) SEM surface images of PDA/PAN supports; (d) SEM surface images of SCOF/PDA/PAN membranes.

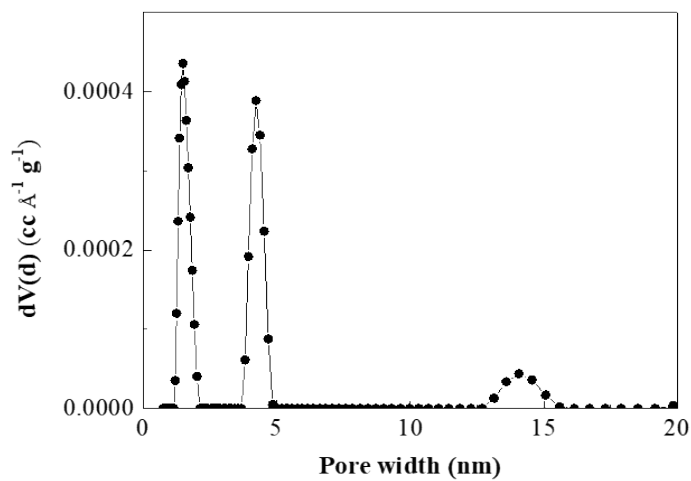


Fig. S8 Pore size distribution of SCOF/PDA(1)/PAN membrane (3#) (DFT method).

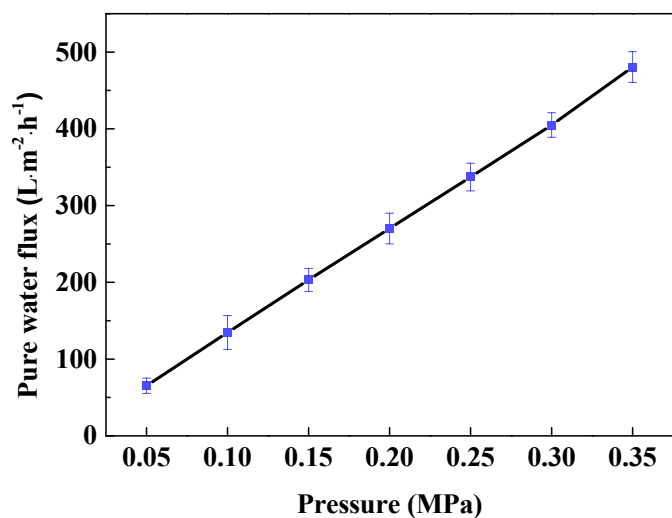


Fig. S9 The compaction resistance of SCOF/PDA(1)/PAN membrane (3#) stabilized for 30 min for different pressure.

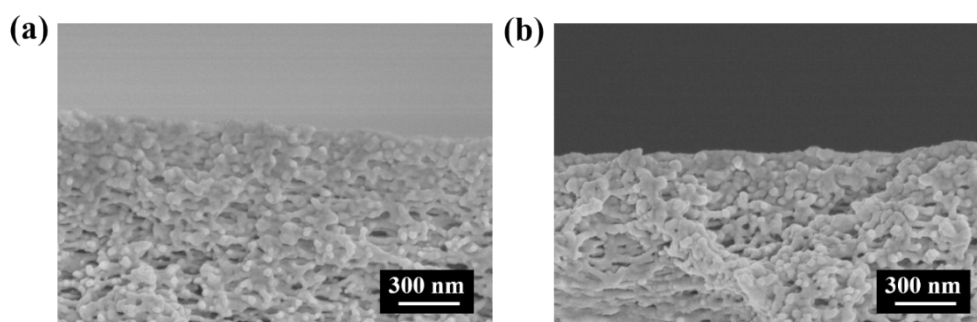


Fig. S10 Cross-section SEM morphology of (a) PAN support and (b) PDA(1)/PAN support.

We also investigated the effects of monomer concentration on membrane structure and performance after determining the optimal PDA coating time of 1 h. As shown in Fig. S11a, homogeneous orange color was observed across the surface of SCOF/PDA/PAN membrane. However, the orange color became a little darker but not obvious with the increase of monomer concentrations, indicating more SCOF crystallites were formed on the support^[S4]. The thickness change of the selective layer (Fig. S11c) confirmed formation of more SCOF crystallites as monomer concentration increased. The morphology of SCOF crystallites almost looked the same along with the change of monomer concentration.

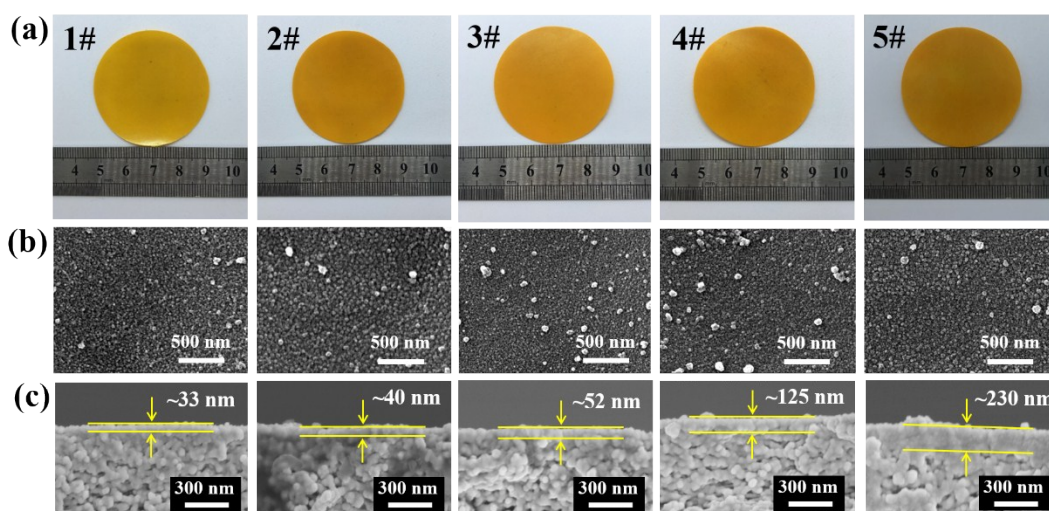


Fig. S11 (a) Digital photographs of membranes 1#-5#; (b) Surface SEM morphology of membranes 1#-5#; (c) Cross-section SEM morphology of membranes 1#-5#.

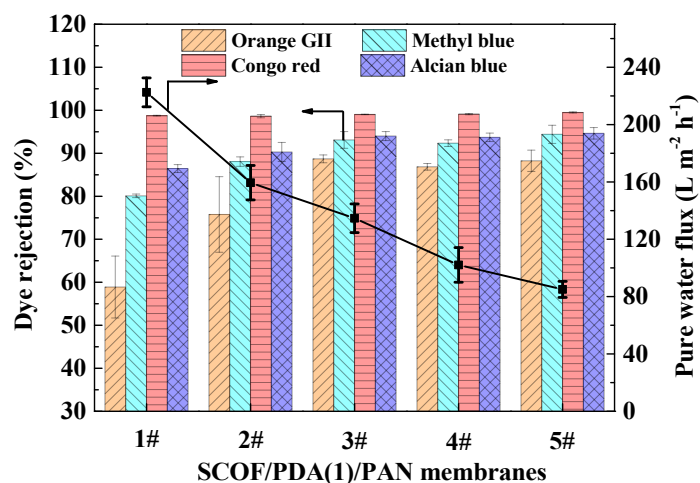


Fig. S12 Performance of the SCO/PDA/PAN membranes with different monomer concentration. (Testing condition: 100 ppm dye solutions at 0.1 MPa; 13.4 cm² effective membrane area; 25 °C; each above value was based on the average of at least five independent membranes).

Static adsorption test of Eriochrome black T by SCO/PDA(1)/PAN membrane was conducted as well. As shown in Fig. S13, the concentration of Eriochrome black T only decreased by 14.4% after 120-h static adsorption at room temperature (25 °C), indicating little dye adsorption of the membrane. Besides, dye adsorption of the thin SCO layer on the PAN support will be quickly saturated. However, as shown in Fig. 7b, the rejection remained above 99% during long-term operation for 100 h. From the above, size exclusion instead of adsorption is the main mechanism for the dye removal of the SCO/PDA(1)/PAN membranes.

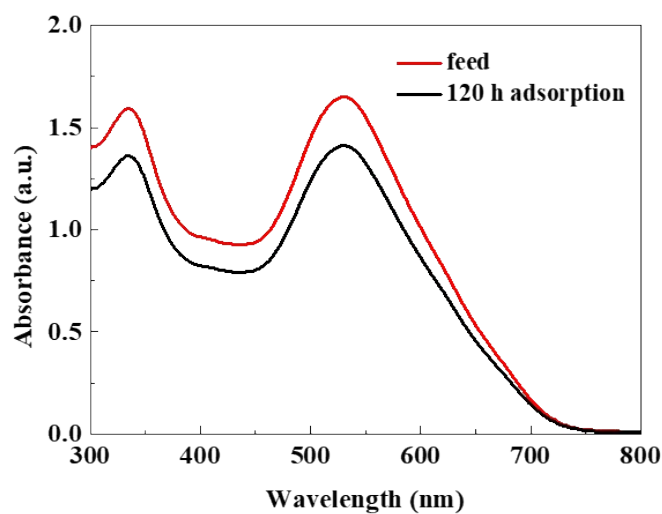


Fig. S13 The static adsorption of SCO/PDA(1)/PAN membrane to Eriochrome black T molecules for 120 h.

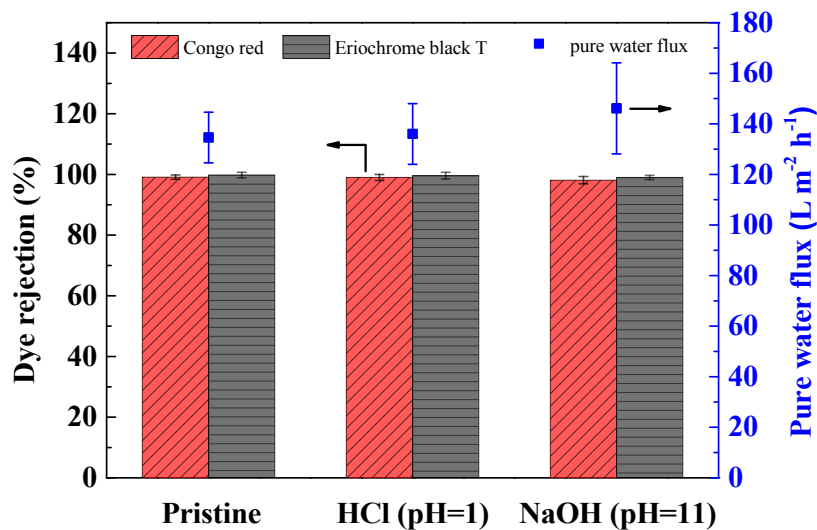


Fig. S14 Chemical stability: separation performance versus harsh treatment of SCOF/PDA(1)/PAN membranes.

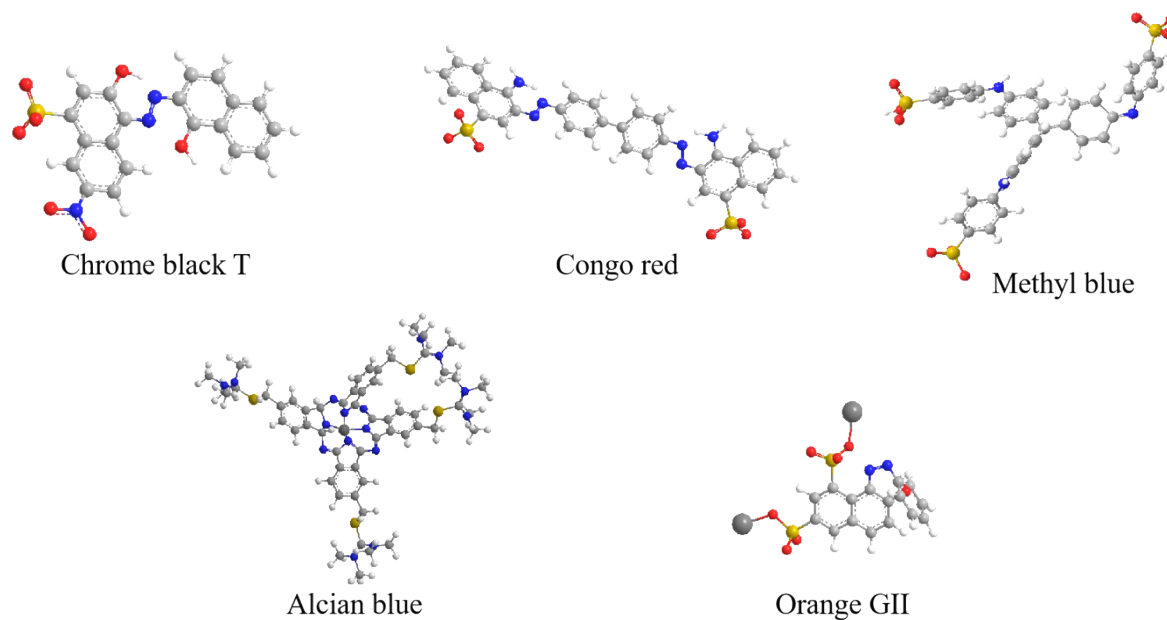


Fig. S15 The molecular model of different dyes used in this work.

Table S2 Characteristics and properties of the water-soluble dye molecules used for the membranes performance tests.

Dye molecule	Charge	M _w	λ _{max}	Molecule size *
Chrome black T	-	461.38	530	1.55 nm×0.88 nm
Congo red	-	696.68	504	2.56 nm×0.73 nm
Methyl blue	-	799.80	580	2.36 nm×1.74 nm
Alcian blue	+	1298.88	331	2.22 nm×2.08 nm
Orange GII	-	452.37	485	1.26 nm×0.92 nm

Note: *Molecule size was measured by material calculation software and quoted from references^[S5-S6].

Table S3 Performance comparison of various membranes towards dyes rejection.

Membrane type	Dye molecule	Permeance (L m ⁻² h ⁻¹ MPa ⁻¹)	Rejection (%)	Operation pressure (bar)	Ref.
---------------	--------------	---	---------------	-----------------------------	------

PEI/CMCNa/PP	Brilliant green	137	99.8	3	[S7]
	Victoria blue B	128	99.6		
	Congo red	57	99.4		
	Crystal violet	134	97.9		
	Rhodamine B	119	98.0		
	Neutral red	107	78.5		
PVDF-SAN-60	Congo red	95	97.5	4	[S8]
	Reactive black 5	104.9	75.0	4	
PAA/PVA/GA	Congo red	42	96	6	[S9]
DEA-modified PA-TFC	Congo red	157.4	99.6	5	[S10]
Co-NF-2	Congo red	182	99.5	8	[S11]
Sepro NF 6	Congo red	133	99.93	6	[S12]
Sepro NF 2A	Congo red	95.85	99.96	6	[S12]
Sericin-TMC	Congo red	135	99.8	5	[S13]
SiO ₂ -PSS/PES	Congo red	252.25	99.8	4	[S14]
CMCNa/PP	Congo red	99	99.8	3	[S15]
	Methyl blue	8.25	99.75	8	
Mineralized PAN	Congo red	255	98	1	[S16]
PEI-GO/PAA/PVA/GA	Methyl blue	8.7	99.3	5	[S17]
Cross-linked PAN/Boltorn	Methyl blue	108.6	97.6	5	[S18]
Modified PEI/PAN	Methyl blue	255	97.3	2	[S19]
TA-GOQD/PAN	Methyl blue	116.5	97.6	2	[S20]
LM-3	Reactive red	145.1	98.9	4	[S21]
ZIF-8/PES	Rose bengal	13	98.95	--	[S22]
Ceramic NF	Chrome black T	247.5	>96.8	3	[S23]
F127/PES	Alcian blue	176.2	95.7	2	[S24]
TA/TMC	Orange GII	168	99.7	2	[S25]
PES-TA (M-60)	Methyl Green	37.2	99.9	5	[S26]
PES-SPMA	Reactive red	145	98	4	[S27]
(NaSS-AC)/PS	Acid red	58	96	4	[S28]
POSS-PDA/PAN	Congo red	1099	98.0	1	[S29]
ZIF-8/PA	Congo red	22.6	99.98	30	[S30]
ZIF-8/PSS	Methyl blue	265	98.6	5	[S31]
ZIF-12/PAN	Methyl blue	272	99.4	2	[S32]
uGNMs	Direct red 81	218.1	99.9	5	[S33]
GO/MoS ₂	Methyl blue	102	97.4	2	[S34]
GO NFM	Evans blue	202.3	98.68	1	[S35]
GO/PAN	Methyl orange	152	97.1	2	[S36]
COF-LZU1	Acid fuchsin	580.5	91.4	5	[S37]
TpPa/PSf	Congo red	500	99.5	3	[S4]
	Methyl blue	500	94.4	3	
TpPa-1/HPAN	Orange GII	418.5	93.91	1	[S1]
TpPa/AAO	Acid fuchsin	140	93.5	0.5	[S38]
SCOF/PDA/PAN	Congo red	1346	99.1	1	This work
	Eriochrome black T	1346	99.2	1	

References

- [S1] F. Pan, W. Guo, Y. Su, N. Khan, H. Yang and Z. Jiang, *Sep. Purif. Technol.*, 2019, 215, 582-589.
- [S2] L. Valentino, M. Matsumoto, W.R. Dichtel and B. J. Mariñas, *Environ. Sci. Technol.* 2017, 51, 14352-14359.
- [S3] M. Matsumoto, L. Valentino, G.M. Stiehl, H.B. Balch, A.R. Corcos, F. Wang, D.C. Ralph, B.J. Mariñas and W.R. Dichtel, *Chem.*, 2018, 4, 308-317.
- [S4] R. Wang, X. Shi, A. Xiao, W. Zhou and Y. Wang, *J. Membr. Sci.*, 2018, 566, 197-204.
- [S5] S. Kandambeth, B. Biswal, H. Chaudhari, K. Rout, S. Kunjattu, S. Mitra, S. Karak, A. Das, R. Mukherjee, U. Kharul and R. Banerjee, *Adv. Mater.*, 2017, 29, 1603945.
- [S6] S. Karan, Z. Jiang, A. Livingston, *Science*, 2015, 348, 1347-1351.
- [S7] Q. Chen, P. Yu, W. Huang, S. Yu, M. Liu and C. Gao, *J. Membr. Sci.*, 2015, 492, 312-321.
- [S8] H. Srivastava, G. Arthanareeswaran, N. Anantharamana and V. Starobv, *Desalination*, 2011, 282, 87-94.
- [S9] L. Wang, N. Wang, G. Zhang and S. Ji, *AIChE Journal*, 2013, 59, 3834-3842.
- [S10] M. Liu, Q. Chen, K. Lu, W. Huang, Z. Lü, C. Zhou, S. Yu and C. Gao, *Sep. Purif. Technol.*, 2017, 173, 135-143.
- [S11] J. Zhu, A. Uliana, J. Wang and S. Yuan, *J. Mater. Chem. A*, 2016, 4, 13211-13222.
- [S12] J. Lin, W. Ye, H. Zeng, H. Yang, J. Shen, S. Darvishmanesh, P. Luis, A. Sotto and B. Bruggen, *J. Membr. Sci.*, 2015, 477, 183-193.
- [S13] C. Zhou, Y. Shi, C. Sun, S. Yu, M. Liu and C. Gao, *J. Membr. Sci.*, 2014, 471, 381-391.
- [S14] L. Xing, N. Guo, Y. Zhang, H. Zhang and J. Liu, *Sep. Purif. Technol.*, 2015, 146, 50-59.
- [S15] S. Yu, Z. Chen, Q. Cheng, Z. Lü, M. Liu and C. Gao, *Sep. Purif. Technol.*, 2012, 88, 121-129.
- [S16] X. Chen, L. Wan, Q. Wu, S. Zhi and Z. Xu, *J. Membr. Sci.*, 2013, 441, 112-119.
- [S17] N. Wang, S. Ji, G. Zhang, J. Li and L. Wang, *Chem. Eng. J.*, 2012, 213, 318-329.
- [S18] L. Wang, S. Ji, N. Wang, R. Zhang, G. Zhang and J. Li, *J. Membr. Sci.*, 2014, 452, 143-151.
- [S19] S. Zhao and Z. Wang, *J. Membr. Sci.*, 2017, 524, 214-224.
- [S20] C. Zhang, K. Wei, W. Zhang, Y. Bai, Y. Sun and J. Gu, *ACS Appl. Mater. Interfaces*, 2017, 9, 11082-11094.
- [S21] J. Wang, L. Qin, J. Lin, J. Zhu, Y. Zhang, J. Liu and B. Bruggen, *Chem. Eng. J.*, 2017, 323, 56-63.
- [S22] Y. Li, L. Wee, A. Volodin, J. Martens and I. Vankelecom, *Chem. Commun.*, 2015, 51, 918-920.
- [S23] P. Chen, X. Ma, Z. Zhong, F. Zhang, W. Xing and Y. Fan, *Desalination*, 2017, 404, 102-111.
- [S24] Y. Zhang, Y. Su, W. Chen, J. Peng, Y. Dong and Z. Jiang, *Ind. Eng. Chem. Res.*, 2011, 50, 4678-4685.
- [S25] Y. Zhang, Y. Su, J. Peng, X. Zhao, J. Liu, J. Zhao and Z. Jiang, *J. Membr. Sci.*, 2013, 429, 235-242.
- [S26] Q. Zhang, H. Wang, S. Zhang and L. Dai, *J. Membr. Sci.*, 2011, 375, 191-197.
- [S27] A. Reddy, J. Trivedi, C. Devmurari, D. Mohan, P. Singh, A. Rao, S. Joshi and P. Ghosh, *Desalination*, 2005, 183, 301-306.
- [S28] A. Akbaria, S.Desclaux, J. Rouch, P. Aptel and J. Remigy, *J. Membr. Sci.*, 2006, 286, 342-350.
- [S29] X. You, H. Wu, Y. Su, J. Yuan, R. Zhang, Q. Yu, M. Wu, Z. Jiang and X. Cao, *J. Mater. Chem. A*, 2018, 6, 13191-13202.
- [S30] L. Wang, M. Fang, J. Liu and J. He, *RSC Adv.*, 2015, 5, 50942-50954.
- [S31] R. Zhang, S. Ji, N. Wang, L. Wang, G. Zhang and J. Li, *Angew. Chem. Int. Ed.*, 2014, 53, 9775-9779.
- [S32] N. Wang, X. Li, L. Wang, L. Zhang, G. Zhang and S. Ji, *ACS Appl. Mater. Interfaces*, 2016, 8, 21979-21983.
- [S33] Y. Han, Z. Xu and C. Gao, *Adv. Funct. Mater.*, 2013, 23, 3693-3700.
- [S34] P. Zhang, J. Gong, G. Zeng, B. Song, W. Cao, H. Liu, S. Huan and P. Peng, *J. Membr. Sci.*, 2019, 574, 112-123.
- [S35] L.Chen, J. Moon, X. Ma, L. Zhang, Q. Chen, L. Chen, R. Peng, P. Si, J. Feng, Y. Li, J. Lou and L. Ci, *Carbon*, 2018, 130, 487-494.
- [S36] M.Zhang, J. Sun, Y. Mao and G. Ping, *J. Membr. Sci.*, 2019, 574, 196-204.
- [S37] H. Fan, J. Gu, H. Meng, A. Knebel and J. Caro, *Angew. Chem. Int. Ed.*, 2018, 57, 4083-4087.
- [S38] X. Shi, A. Xiao, C. Zhang and Y. Wang, *J. Membr. Sci.*, 2019, 576, 116-122.